Spatially localized modes in two-dimensional chirped photonic lattices

Mario I. Molina,[1,2,3] Yaroslav V. Kartashov,[2] Lluis Torner,[2] and Yuri S. Kivshar[3]
[1]*Departamento de Física, Facultad de Ciencias, Universidad de Chile, Casilla 653, Santiago, Chile*
[2]*ICFO-Institut de Ciencies Fotoniques and Universitat Politecnica de Catalunya, Mediterranean Technology Park, 08860 Castelldefels, Barcelona, Spain*
[3]*Nonlinear Physics Center, Research School of Physical Sciences and Engineering, Australian National University, Canberra, ACT 0200, Australia*

We numerically study both linear and nonlinear surface modes in semi-infinite chirped two-dimensional photonic lattices in the framework of an effective discrete nonlinear model. We demonstrate that the lattice chirp can dramatically change the conditions for the mode localization near the surface even in the linear limit, and we find surface modes, in linear lattices, and the families of discrete surface solitons, in nonlinear lattices. In a sharp contrast to one-dimensional discrete surface solitons, we demonstrate that the mode threshold power in two-dimensional lattices is lowered by the action of both the surface and lattice chirp. By manipulating the lattice chirp, we can control the mode position and its localization.

I. INTRODUCTION

In linear guided-wave optics, surface states have been predicted to exist at interfaces separating periodic and homogeneous dielectric media [1]. The interest in the study of surface states has been renewed recently because an interplay of self-focusing nonlinearity and repulsive effect of the surface was shown to facilitate the formation of discrete surface solitons located at the edge of the waveguide array [2,3]. The existence and main properties of surface solitons can be understood with a simple physics as localization of discrete optical solitons near the surface when the mode power exceeds a certain threshold value, compensating the repulsive action of the surface by the nonlinear trapping due to discreteness [4]. A similar effect of the light localization near the edge of the waveguide array and the formation of surface gap solitons has been predicted theoretically [2,5] and observed experimentally [6,7] for truncated arrays of defocusing nonlinear waveguides.

Recent studies [8] demonstrated that the conditions for the formation of surface solitons can be dramatically modified near the surface of a chirped optical lattice. Due to combined actions of internal reflection at the interface, distributed Bragg-type reflection and focusing nonlinearity, it was found that surfaces of chirped lattices become soliton attractors, in sharp contrast to standard unchirped lattices. The conclusions of these studies were later confirmed in the framework of a discrete model [9].

It is important to analyze how the properties of nonlinear surface waves are modified by the lattice dimensionality. The first studies of different types of discrete surface solitons in two-dimensional nonlinear photonic lattices [10–14] revealed, in particular, that the presence of a surface increases the stability region for two-dimensional discrete solitons [13], and the threshold power for the edge surface state is slightly higher than that for the corner soliton [12,14]. Recent observations of two-dimensional surface solitons in optically induced photonic lattices [15] and laser-written waveguide arrays in fused silica [16] demonstrated novel features of these nonlinear surface modes in comparison with their counterparts in one-dimensional waveguide arrays.

In this paper, we employ a two-dimensional discrete model of a chirped photonic lattice to provide a deeper physical insight into the properties of linear surface modes and discrete surface solitons in chirped photonic lattices. In particular, we demonstrate that a critical value of the lattice chirp is necessary for the existence of a linear mode localized at the surface. Above this threshold value, the surface solitons originate from the corresponding linear surface modes, and they do not require any threshold power for their existence. We study the dependence of the mode position near the surface and the critical power as a function of the lattice chirp, and also demonstrate how the engineered chirp of the photonic lattice can facilitate a selective nonlinear localization near the surface.

The paper is organized as follows. In Sec. II we introduce our discrete nonlinear model of a two-dimensional chirped lattice. Section III is devoted to the study of localized modes in linear chirped lattices. In particular, we consider two special cases of the chirp and demonstrate that the chirp can dramatically change the conditions for the mode localization near the surface, so that surface modes may exist even in a linear lattice provided the chirp parameter exceeds some threshold value. In Sec. IV, we study the localization of nonlinear modes near the surface and, in particular, demonstrate that by engineering the lattice chirp we can control the localization of nonlinear modes and their location on the lattice. Finally, Sec. V concludes the paper.

II. MODEL

We consider a two-dimensional array of $N \times N$ nonlinear (Kerr) single-mode waveguides which form a square lattice with the lattice spacing $a(\equiv 1)$. We introduce a spatial chirp into the system by changing the individual refraction index of the guides and/or adjusting the waveguide dimensions. In the first case, both the propagation constant and coupling between the neighboring waveguides become chirped; in the

second case, only the coupling is affected. In particular, it is possible to have a situation where the coupling chirp due to a change of the refraction index is greatly reduced by judicious engineering of the guide transverse dimensions. As a result, only chirp in the propagation constant is relevant in this case. In what follows, we consider both cases separately since they do lead to a different asymptotic behavior.

In the framework of the coupled-mode theory, the nonlinear equations for the amplitudes of the stationary modes can be written in general as

$$-\beta C_{\mathbf{n}} + \lambda_{\mathbf{n}} C_{\mathbf{n}} + \sum_{\mathbf{m}} V_{\mathbf{n},\mathbf{m}} C_{\mathbf{m}} + \gamma |C_{\mathbf{n}}|^2 C_{\mathbf{n}} = 0. \tag{1}$$

For a two-dimensional, semi-infinite square nonlinear lattice, Eq. (1) becomes

$$-\beta C_{n,m} + \lambda_{n,m} C_{n,m} + \sum_{j=\pm 1} V_{(n,m),(n+j,m)} C_{n+j,m} + \sum_{j=\pm 1} V_{(n,m),(n,m+j)} C_{n,m+j} + \gamma |C_{n,m}|^2 C_{n,m} = 0, \tag{2}$$

where $n \geq 0$ and $m \geq 0$, and $V_{(n,m),(n',m')} = 0$ if either $n' < 0$ or $m' < 0$.

We now modulate the refraction index $\rho(n,m)$ of each guide to decrease it exponentially away from the corner site (0, 0), in a general, anisotropic manner:

$$\rho(n,m) = \rho_0 \exp(-\sigma_x n - \sigma_y m), \tag{3}$$

where σ_x and σ_y are two chirp parameters in the x and y direction, respectively. This change in the refraction index affects the effective propagation constant of each guide in a similar way,

$$\lambda_{n,m} = \lambda_0 \exp(-\sigma_x n - \sigma_y m). \tag{4}$$

In principle, the couplings between the neighboring waveguides are also affected by the chirp. If the chirp in the refraction index varies slowly in space then, to first-order approximation, the waveguide couplings is affected in the same way:

$$V_{(n,m),(n+1,m)} = V_0 \exp(-\sigma_x n - \sigma_y m) = V_{(n,m),(n,m+1)},$$

$$V_{(n,m),(n-1,m)} = V_0 \exp[-\sigma_x (n-1) - \sigma_y m],$$

$$V_{(n,m),(n,m-1)} = V_0 \exp[-\sigma_x n - \sigma_y (m-1)].$$

However, since the coupling between the waveguides also depends upon an overlap of the mode fields, it is possible in principle to engineer the waveguide parameters judiciously in order to compensate for the spatial variation of the refraction index, rendering the couplings nearly constant: $V_{\mathbf{n},\mathbf{m}} \approx V_0$. Hereafter, we consider both cases separately.

III. LINEAR SURFACE MODES

A. Chirp in the propagation constant

Let us begin by arguing that it is possible, in principle, to have a two-dimensional array of waveguides, where the chirp in refraction index affects only the propagation constants, leaving the couplings nearly unchanged. According to conventional coupled-mode theory [17,18], for two identical couplers, say two dielectric cylinders of index n, radius a, separated by a distance d between their centers and embedded in a uniform medium with refraction index $n_b < n$, their coupling coefficient V depends in a rather complex manner on the guide parameters. However, in the limit of weak coupling, the dependence of V on the various parameters is approximately

$$aV \propto (n^2 - n_b^2)^{1/2} \frac{1}{\sqrt{d/a}} e^{-w(d/a)}, \tag{5}$$

where w is the solution of a transcendental equation. While this applies to two identical fibers in solation, it should still be qualitatively valid for a two-dimensional array of weakly coupled guides, if we assume a weak chirp of the guide indices. Therefore it would be possible to compensate for a chirp in n by adjusting either the distance d or the guide radius a. Since in our case we are dealing with a two-dimensional situation, simply adjusting the distances between neighboring guides is not possible because we have to adjust in two directions at the same time. Thus we resort to a readjustment of the guide radius: if V decreases because of an exponential chirp on the index n, one could compensate by increasing slightly the radius of consecutive guides, in order to render V almost constant. Figure 1 shows a possible configuration array following these ideas, for the case of an isotropic chirp in refraction index [Eq. (3) with $\sigma_x = \sigma_y$].

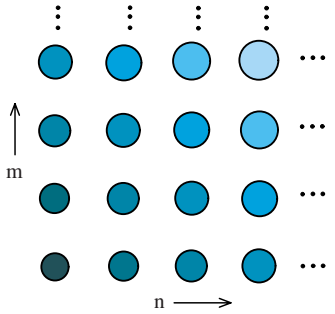

FIG. 1. (Color online). Transverse view of a two-dimensional waveguide array with an exponential chirp on the refractive indices, but nearly constant coupling coefficients. The darker (lighter) shade denotes a higher (lower) index value. The center-to-center distance between guides remains constant. Both the shading contrast and the change in guide dimensions have been exaggerated for ease in visualization.

Thus assuming chirp in the propagation constants only, the equations for the stationary modes have the form

$$\beta C_{n,m} = \lambda_0 \exp(-\sigma_x n - \sigma_y m) C_{n,m} + V_0 \sum_{j=\pm 1} (C_{n+j,m} + C_{n,m+j}) + \gamma |C_{n,m}|^2 C_{n,m}. \tag{6}$$

We start by examining the case of $N \times N$ linear modes ($\gamma = 0$), which is relevant to the case of weak input power $P \equiv \Sigma_{n,m} |C_{n,m}|^2 \ll 1$. For a fixed number of waveguides, we diagonalize the system of discrete linear equations (6) and find

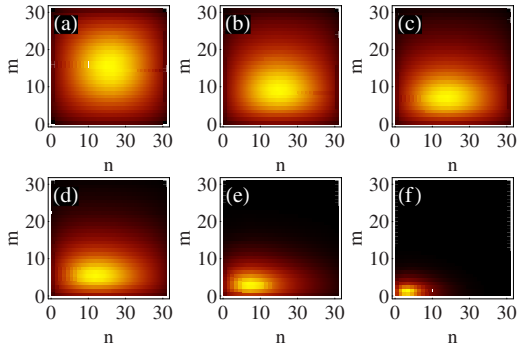

FIG. 2. (Color online). Anisotropic chirp in the propagation constant only: Density profiles of localized nodeless modes for different values of the chirp (σ_x,σ_y) for a 31×31 linear array with $\lambda_0/V_0=5$. (a) (0,0), (b) $(5\times10^{-5},5\times10^{-4})$, (c) $(10^{-4},10^{-3})$, (d) $(2\times10^{-4},2\times10^{-3})$, (e) $(10^{-3},10^{-2})$, and (f) $(10^{-2},10^{-1})$.

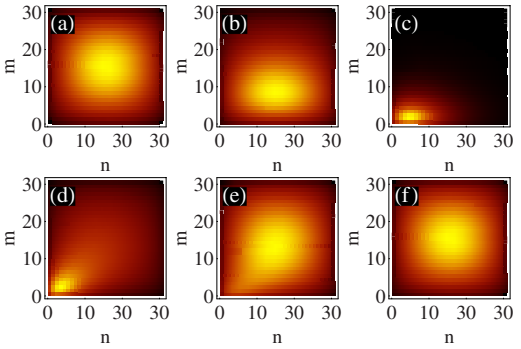

FIG. 3. (Color online). Anisotropic chirp in the propagation constant only: Density profiles of a localized nodeless mode for different values of the chirp (σ_x,σ_y) for $\lambda_0/V_0=1$. (a) (0,0), (b) $(2\times10^{-4},3\times10^{-3})$, (c) $(3\times10^{-2},3\times10^{-1})$, (d) $(2\times10^{-1},5\times10^{-1})$, (e) $(10^{-1},1)$, and (f) (1,1).

all the modes. In particular, we focus on the nodeless (fundamental) mode and how it changes as a function of the chirp parameters σ_x and σ_y. From Eq. (6) we find that, in the limit of large chirp, $\sigma_x,\sigma_y\gg1$, the system reduces to a two-dimensional lattice with a linear impurity at one of the corner sites. It can be proven [19] that in this case for $N\to\infty$, a localized mode centered at the corner site is possible, provided

$$\lambda_0/V_0>[2-(16/3\pi)]^{-1}\equiv(\lambda_0/V_0)_c.$$

Thus two regimes appear: (1) For $\lambda_0/V_0>(\lambda_0/V_0)_c\sim3.3$, an increase in the chirp values shifts the center of the nodeless mode from the center of the lattice toward the corner site. For sufficiently large average chirp, $\langle\sigma\rangle=(1/2)(\sigma_x+\sigma_y)$, the mode center approaches the corner site position and its spatial extension reduces considerably (see Fig. 2). (2) When $\lambda_0/V_0<(\lambda_0/V_0)_c$, the mode center shifts from the center of the lattice toward the corner site upon the average chirp increase as above, but upon further chirp increase, the mode center shifts away from the corner site and it approaches the center of the lattice asymptotically (see Fig. 3).

In order to visualize and quantify this behavior of the mode center as the chirp is increased, we consider the isotropic case $\sigma_x=\sigma_y$ and calculate numerically the mode position relative to the lattice corner along the diagonal (n,n) as a function of the chirp for both cases, $\lambda_0/V_0>(\lambda_0/V_0)_c$ and $\lambda_0/V_0<(\lambda_0/V_0)_c$. The results are shown in Fig. 4. The observed dependence is presented by a series of discrete steps of a widely varying width. At small chirp, the fundamental mode is confined well inside the lattice, and a small change of the chirp can alter the position of the mode maximum considerably. As the mode gets closer to the corner, the steps increase in size. For $\lambda_0/V_0>(\lambda_0/V_0)_c$, the mode finally reaches the corner site where it will remain upon further chirp increase [see Fig. 4(a)]. On the contrary, for $\lambda_0/V_0<(\lambda_0/V_0)_c$, the mode reaches a minimum distance from the corner and, upon further chirp increase, it shifts away from the corner and reaches the middle of the lattice in the limit of very large chirp [see Fig. 4(b)].

B. Chirp in the propagation constant and waveguide coupling

This seems to be a more realistic case that originates from modulation of the refractive index imposed on the periodic square array of coupled waveguides. If the modulation is smooth, then both the propagation constants and waveguide couplings are affected in the same manner. This leads to the following set of coupled equations for the linear modes:

$$\begin{aligned}\beta C_{n,m}=&\,e^{-\sigma_x n-\sigma_y m}[\lambda_0 C_{n,m}+V_0(C_{n+1,m}+C_{n,m+1})]\\&+V_0e^{-\sigma_x n-\sigma_y m}[e^{\sigma_y}C_{n,m-1}+e^{\sigma_x}C_{n-1,m}],\end{aligned}\tag{7}$$

where $C_{n',m'}=0$ if either $n'<0$ or $m'<0$. A candidate waveguide array for this case could be the one shown in Fig. 1, but with all guides with the same radius.

In this case, from Eq. (7) we obtain that, in the limit of a large average chirp, the system becomes an effective trimer. Thus the localized nodeless mode remains in the immediate vicinity of the corner site, and there will not be any bouncing phenomena for the mode center as in the previous section.

As the values of the chirp in both directions are increased from zero, the fundamental mode will shift from the center of the lattice approaching the corner site, as shown in Fig. 5. The precise route of the mode center toward the corner site depends on the values of both σ_x and σ_y. We now perform a numerical sweep in the (σ_x,σ_y) space and record the position (x,y) of the mode maximum. The results for the x position are shown in Fig. 6.

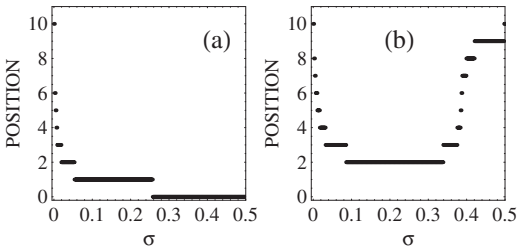

FIG. 4. Distance of the mode maximum from the corner of the array as a function of the chirp parameter, for the isotropic case $\sigma_x=\sigma_y\equiv\sigma$. (a) $\lambda_0/V=5$. (b) $\lambda_0/V=1$.

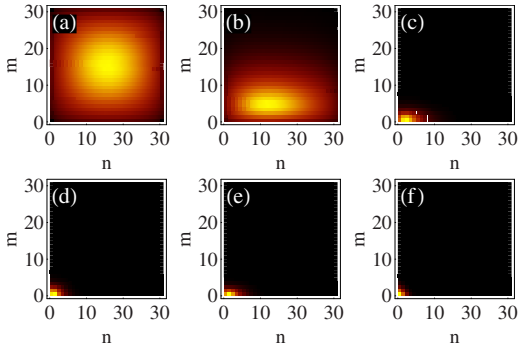

FIG. 5. (Color online). Same as in Fig. 2, but including chirp in propagation constant *and* in waveguide couplings.

Due to symmetry, the position of the y coordinate of the mode maximum can be obtained from the same figure by exchanging σ_x and σ_y. We notice that, at small average chirp value, the mode center is very sensitive to the precise value of the chirps. As chirps are increased, the position of the mode center becomes less sensitive and the width of the "terraces" become larger. For chirp values greater than, say ≈ 0.3, the mode will be centered on the corner site and will remain there upon further chirp increase.

IV. SURFACE SOLITONS IN CHIRPED NONLINEAR LATTICES

Having examined the main features of the fundamental linear (i.e., low power) surface modes in the presence of an anisotropic chirp, we now consider the case of a nonlinear lattice, i.e., $\gamma \neq 0$. We focus on the more interesting case of chirp in both the propagation constant and guide coupling examined in the previous section. The stationary equations now read:

$$\beta C_{n,m} = e^{-\sigma_x n-\sigma_y m}[\lambda_0 C_{n,m} + V_0(C_{n+1,m} + C_{n,m+1})] + V_0 e^{-\sigma_x n-\sigma_y m}[e^{\sigma_y} C_{n,m-1} + e^{\sigma_x} C_{n-1,m}] + \gamma |C_{n,m}|^2 C_{n,m} \quad (8)$$

where $C_{n',m'}=0$ if either $n'<0$ or $m'<0$, and $\gamma=1$. For a given value of β, we solve these equations numerically with the help of a straightforward extension of the multidimensional Newton-Raphson method used earlier in our analysis of the one-dimensional system [9]. To do so, we first present the two-dimensional $N\times N$ system as an effective, N^2-long one-dimensional chain by means of a convenient relabeling of the site coordinates, and then apply the usual Newton-Raphson method [9].

As an example, we consider the linear modes presented in Figs. 5(a)–5(f) and recalculate them in the case of nonlinear lattice ($\gamma=1$). The corresponding results for the nonlinear localized modes are shown in Figs. 7(a)–7(f). We note that, in comparison with the linear modes, the position of the nonlinear mode center does not change, but the spatial extension of the mode is reduced considerably, due to the self-trapping effect.

We now focus on the simplest possible nonlinear surface modes that can be supported by the two-dimensional (2D)

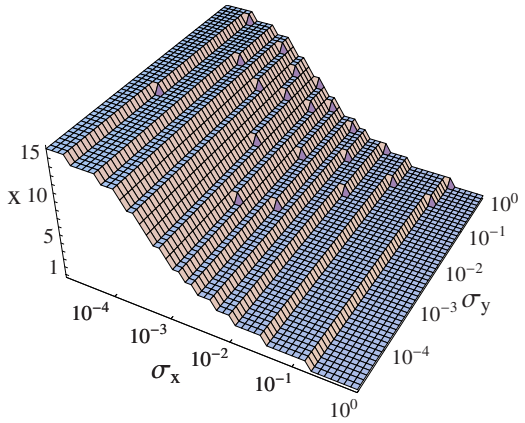

FIG. 6. (Color online). Anisotropic chirp in both the propagation constant and couplings: Position of the center of the nodeless mode along the x coordinate as a function of the chirp parameter for $N=21$ and $\lambda_0/V_0=1$.

lattice in the presence of chirp. Figure 8 below shows plots of power versus propagation constant for surface modes residing at the corner (0, 0) and at the edge $(0,N/2)$ of the lattice, for a symmetrical chirp $\sigma_x=\sigma_y\equiv\sigma$, for different chirp parameter values σ.

For the case of a surface mode centered at a corner site, we have that, due to the symmetry of the chirp, the corner site becomes the origin of a quasi-one-dimensional system as far as chirp is concerned. As a consequence, its power versus propagation constant curves resemble the ones found for a one-dimensional (1D) chirped lattice. In particular, for chirp values above some threshold, the minimum power needed to localize the mode at the corner site drops to zero (see also Fig. 9 below).

The situation for an edge mode is quite different. Due to the form of the chirp function, all couplings (and propagation constants) decrease exponentially away from the corner. This effect is particularly strong for the edge site, especially for large lattices, and causes the edge site to become increasingly decoupled from the rest of the lattice as the chirp increases. As a result, it becomes easier for the edge site to self-trap power than for the corner site, in marked contrast to the case of a 2D lattice without chirp, where the power

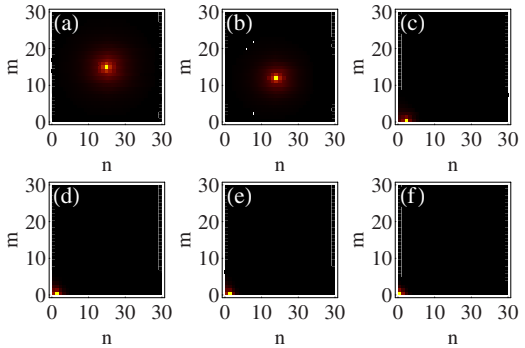

FIG. 7. (Color online). Nonlinear localized modes near the corner of a two-dimensional lattice in the case of an anisotropic chirp in both the propagation constant and couplings. Parameters are the same as in Fig. 5 except for $\gamma=1$.

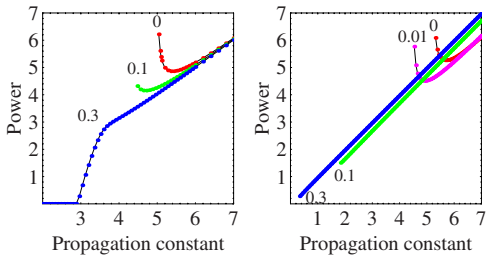

FIG. 8. (Color online). Left (right): Power versus propagation constant of a surface mode centered on a corner (edge) site, for different chirp values, for the case of a symmetric chirp: $\sigma_x=\sigma_y \equiv \sigma$. The numbers on each curve denote the value of chirp σ ($N=31$).

needed to effect a surface mode is lower for a corner site than for an edge site. As a result, the equations for the edge site quickly converge to $\beta \approx |C_{0,N/2}|^2$ upon chirp increase, and the power vs propagation constant curves will approach the straight line $\beta=P$. This behavior is clearly seen in Fig. 8 for chirp values above $\sigma \approx 0.1$.

Next, we compute the minimum power needed to create a nonlinear localized mode at the corner site, for arbitrary values of the chirp parameters (σ_x, σ_y). Results are shown in Fig. 9. As expected (Fig. 8), at small average values of the lattice chirp, a minimum power is needed to create a stable mode, while above a certain value of the chirp no minimum power is required, similar to the case of a one-dimensional chirped lattice [9]. The power surface decreases slowly with average chirp, until one reaches the lines $\sigma_x \sim 0.3$ and $\sigma_y \sim 0.3$, where there is an abrupt drop to zero power level.

By combining all the information gathered so far on stationary modes, linear and nonlinear, we realize that, by changing either the lattice chirp or the effective nonlinearity, we can control not only the mode localization but also its location in the lattice near the surface. This property provides an efficient physical mechanism for the low-power generation of nonlinear localized modes near lattice surfaces and other defects, where the threshold power for the generation of the nonlinear localized mode is lower than in a bulk. It is now possible to move the localized mode in a given direction to a desired position on the lattice by engineering both the

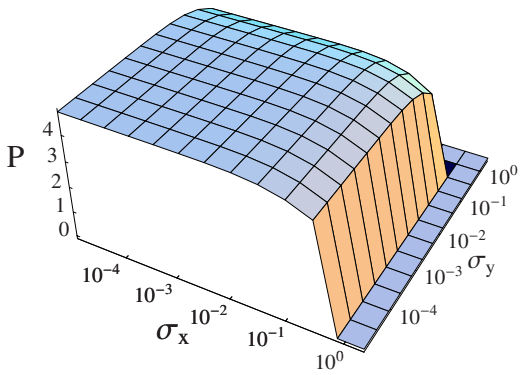

FIG. 9. (Color online). Anisotropic chirp in both the propagation constant and couplings: Minimum power for creating a nonlinear localized surface mode at the lattice corner, as a function of the chirp parameters (σ_x, σ_y) for $\lambda_0/V=1$.

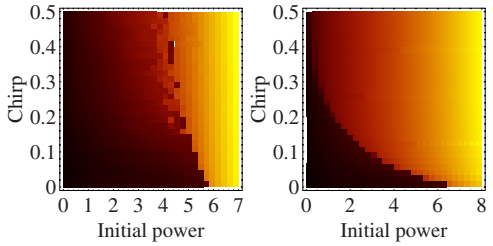

FIG. 10. (Color online). Left (right): Average output power at a corner (edge) site, as a function of chirp value and initial power at a corner (edge) site. ($\sigma_x=\sigma_y \equiv \sigma$).

value and direction of the lattice chirp, and then localize the mode by further increasing the nonlinearity. As a matter of fact, this simple mechanism is presented in Figs. 5(a)–5(f) and Figs. 7(a)–7(f). However, since this scheme requires an input beam in the shape of the fundamental mode, it can be practical for small waveguide arrays only. This brings us to the question of possible mobility of narrow discrete solitons in our system. In fact, for a 1D waveguide array with Kerr nonlinearity it was proven possible to engineer a judicious coupling chirp with a completely predictable soliton steering [20,21].

Therefore we consider next the dynamical evolution of an initial input beam, in the presence of chirp and nonlinearity. Our numerical computations show that localized nonlinear excitations have no mobility, regardless of the chirp value, in agreement with previous results for unchirped 2D systems with Kerr nonlinearity. As a result, we choose to focus on the excitation of a surface mode by a completely localized input beam of power P: $A_{nm}(0)=\sqrt{P}\delta_{n_0,m_0}$, where (n_0, m_0) is the center position of a surface guide, in the presence of chirp. After some evolution distance $z_{\max}$, we compute the average amount of power remaining on the initial launching guide at (n_0, m_0):

$$\langle P_0 \rangle = \frac{1}{z_{\max}} \int_0^{z_{\max}} |A_{n_0,m_0}(z)|^2 dz,$$

and plot the dependence of $\langle P_0 \rangle$ on chirp and initial power P. Results are shown in Fig. 10 for the symmetrical chirp case ($\sigma_x=\sigma_y$), for the corner $n_0=m_0=0$, and edge $n_0=0, m_0=N/2$ cases.

The first observation is that, for a finite chirp value, it seems easier to dynamically excite an edge mode than a corner mode. This is only consistent with the earlier observation that the edge site is substantially more decoupled from the lattice than the corner site, due to the specific form of the chirp function. In the limit of a small chirp, however, it is always easier to excite a corner mode than an edge one, as Fig. 10 shows. Another general observation is that, as chirp values increase, it becomes easier for the system to self-trap power at the launching guides. However, since an increase in chirp tends to diminish the effective size N_{eff} of the array *via* the increasing decoupling of the sites, the sharpness of the self-trapping transition tends to decrease with chirp increase. For a large enough chirp, the effective system is so small that even in the diffraction regime ($P \to 0$), $1/N_{\text{eff}}$ is substantially

larger than zero causing a sort of linear trapping. Also, in this regime the fluctuations are large due to the trapped radiation that remains bouncing back and forth in the vicinity of the launching point and $\langle P_0 \rangle$ becomes less useful. These fluctuations are more noticeable for the corner site than the edge site case, since in the limit of large chirp, the system reduces to a trimer and an isolated site, respectively. Of course, in the high power limit, usual self-trapping dominates and virtually all of the power remains at the original launching guides. We have examined other intermediate cases, e.g., the case of an asymmetrical chirp $\sigma_x = \sigma, \sigma_y = (1/2)\sigma$, with results consistent with the above observations.

V. CONCLUSIONS

We have analyzed numerically both surface modes and discrete surface solitons in two-dimensional chirped linear and nonlinear photonic lattices, in the framework of an effective two-dimensional discrete model. We have demonstrated that the lattice chirp can dramatically change the conditions for the mode localization near the surface even in the linear case, and we have found numerically linear surface modes and discrete surface solitons. We have demonstrated that by manipulating the lattice chirp, we can control not only the mode localization, but also its location in the lattice near the surface. This provides an efficient tool for the low-power generation of nonlinear localized modes and their control for finite waveguide arrays. We believe the basic principles of engineering the localization of linear and nonlinear localized modes in chirped lattices can be soon verified experimentally, and the general concept will be useful for its implementation in other discrete nonlinear systems.

ACKNOWLEDGMENTS

This work has been supported by Fondecyt Grants No. 1050193 and No. 7050173 in Chile, and by the Australian Research Council in Australia. M.I.M. thanks ICFO-Institut de Ciencies Fotoniques (Barcelona) and the Nonlinear Physics Center at the Australian National University for hospitality and support.

[1] P. Yeh, A. Yariv, and A. Y. Cho, Appl. Phys. Lett. **32**, 102 (1978).
[2] K. G. Makris, S. Suntsov, D. N. Christodoulides, G. I. Stegeman, and A. Haché, Opt. Lett. **30**, 2466 (2005).
[3] S. Suntsov, K. G. Makris, D. N. Christodoulides, G. I. Stegeman, A. Haché, R. Morandotti, H. Yang, G. Salamo, and M. Sorel, Phys. Rev. Lett. **96**, 063901 (2006).
[4] M. I. Molina, R. A. Vicencio, and Yu. S. Kivshar, Opt. Lett. **31**, 1693 (2006).
[5] Y. V. Kartashov, L. Torner, and V. A. Vysloukh, Phys. Rev. Lett. **96**, 073901 (2006).
[6] C. R. Rosberg, D. N. Neshev, W. Krolikowski, A. Mitchell, R. A. Vicencio, M. I. Molina, and Yu. S. Kivshar, Phys. Rev. Lett. **97**, 083901 (2006).
[7] E. Smirnov, M. Stepić, C. E. Rütter, D. Kip, and V. Shandarov, Opt. Lett. **31**, 2338 (2006).
[8] Y. V. Kartashov, V. A. Vysloukh, and L. Torner, Phys. Rev. A **76**, 013831 (2007).
[9] M. I. Molina, Y. V. Kartashov, L. Torner, and Yu. S. Kivshar, Opt. Lett. **32**, 2668 (2007).
[10] Y. V. Kartashov and L. Torner, Opt. Lett. **31**, 2172 (2006).
[11] Y. V. Kartashov, V. A. Vysloukh, D. Mihalache, and L. Torner, Opt. Lett. **31**, 2329 (2006).
[12] K. G. Makris, J. Hudock, D. N. Christodoulides, G. I. Stegeman, O. Manela, and M. Segev, Opt. Lett. **31**, 2774 (2006).
[13] H. Susanto, P. G. Kevrekidis, B. A. Malomed, R. Carretero-Gonzalez, and D. J. Frantzeskakis, Phys. Rev. E **75**, 056605 (2007).
[14] R. A. Vicencio, S. Flach, M. I. Molina, and Yu. S. Kivshar, Phys. Lett. A **364**, 274 (2007).
[15] X. Wang, A. Bezryadina, Z. Chen, K. G. Makris, D. N. Christodoulides, and G. I. Stegeman, Phys. Rev. Lett. **98**, 123903 (2007).
[16] A. Szameit, Y. V. Kartashov, F. Dreisow, T. Pertsch, S. Nolte, A. Tünnermann, and L. Torner, Phys. Rev. Lett. **98**, 173903 (2007).
[17] A. W. Snyder, J. Opt. Soc. Am. **62**, 1267 (1972).
[18] Katsunari Okamoto, *Fundamentals of Optical Waveguides* (Academic, New York, 2005).
[19] M. I. Molina, Phys. Rev. B **74**, 045412 (2006).
[20] R. A. Vicencio, M. I. Molina, and Yu. S. Kivshar, Opt. Lett. **28**, 1942 (2003).
[21] A. Fratalocchi, G. Assanto, K. A. Brzakiewicz, and M. A. Karpierz, Appl. Phys. Lett. **86**, 051112 (2005).